

More About This Article

Additional resources and features associated with this article are available within the HTML version:

- Supporting Information
- Links to the 5 articles that cite this article, as of the time of this article download
- Access to high resolution figures
- Links to articles and content related to this article
- Copyright permission to reproduce figures and/or text from this article

[View the Full Text HTML](#)



Three-Coordinate Metal Centers in Extended Transition Metal Oxides

Amy Bowman,[†] Mathieu Allix,[†] Denis Pelloquin,[‡] and Matthew J. Rosseinsky^{*†}

Department of Chemistry, University of Liverpool, Liverpool L69 7ZD, United Kingdom, and
Laboratoire CRISMAT-ENSICAEN, UMR6508, 6 Bd du Maréchal Juin, 14050 Caen Cedex, France

Received June 9, 2006; E-mail: m.j.rosseinsky@liverpool.ac.uk

Transition metal oxides able to withstand variable oxygen partial pressure environments are of considerable current interest as solid oxide fuel cell electrodes¹ and gas separation membranes.² To perform the function of transporting both ions and electrons required for these applications, such materials need to maintain both mobile oxygen vacancies or interstitials and metal oxidation states corresponding to partly filled d-bands over a wide oxygen partial pressure range. This requires the ability to accommodate a range of metal coordination environments and oxidation states. Perovskites of iron and cobalt in the (La,Sr)(Fe,Co)O₃ family have been extensively studied for their mixed ionic and electronic conductivity in ceramic membrane applications.² The related Ruddlesden–Popper (RP) A_{n+1}B_nO_{3n+1} materials derived by inserting excess (La,Sr)O rock-salt layers between *n* – octahedra thick perovskite blocks have recently attracted attention due to their enhanced stability in reducing environments, with in situ neutron powder diffraction demonstrating that these phases form when the *n* = ∞ ABO₃ perovskites are reduced at and below 10^{−14} atm O₂ at 900 °C and are stable to the reducing atmosphere.³ Here we show that the *n* = 3 RP phase Sr₃LaFe_{1.5}Co_{1.5}O_{10.1}⁴ is capable of sustaining O contents as low as O_{7.5} with a mean metal oxidation state of +2 and three coordination at the central site in the trilayer of originally octahedral transition metal sites.

Sr₃LaFe_{1.5}Co_{1.5}O_{10.1} **I** adopts the *n* = 3 RP structure with three layers of untilted corner-sharing octahedra separated by a rock-salt layer (Figure 1a). Neutron and X-ray powder diffraction reveal no ordering of Fe and Co over the two (central Fe/Co1 and terminal Fe/Co2) B sites or of La and Sr on the A sites. Reduction of **I** in a stream of 5% H₂/N₂ (Figure S1a) reveals a mass-loss plateau at 500–800 °C corresponding to the formation of the reduced phase Sr₃LaFe_{1.5}Co_{1.5}O_{8.25} **II**, confirmed by iodometric titration in addition to the observed mass loss. The composition of **II** corresponds to a mean B site oxidation state of +2.5, with the chemically reasonable assignments of Fe³⁺ and Co²⁺. Reduction produces a notable elongation in the *c* lattice parameter and a smaller increase in *a*. Reduction of **I** with the more powerful hydride reducing agent CaH₂⁵ produces a different outcome. In situ observation of the reaction by X-ray diffraction (Figure S2) reveals the onset of the formation of a reduced phase at 300 °C which differs from **II** as signaled by relative elongation of *c* and decrease in *a*. Reaction with CaH₂ in a sealed tube at 450 °C and subsequent removal of byproducts affords **III**, with an oxygen content determined by TG reoxidation (Figure S1b) of Sr₃LaFe_{1.5}Co_{1.5}O_{7.49}, corresponding to removal of 25% of the original anions. This gives a mean B site oxidation state of +2, with both Fe and Co adopting the same oxidation state. X-ray absorption spectroscopy (Figure S3) shows that both metals are further reduced than in **II**, suggesting reduction of Co to below +II. EDX analysis of **III** in the TEM reveals that

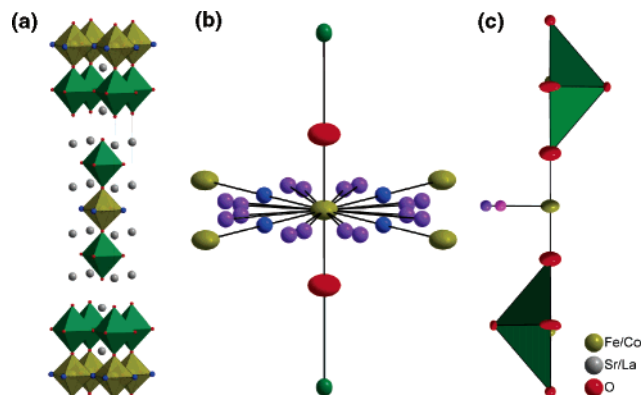


Figure 1. (a) The *n* = 3 RP structure (space group *I4/mmm*) of **I** LaSr₃(Fe_{1.5}Co_{1.5})O₁₀ – the O5 anions removed to form **III** are shown in blue. The central Fe/Co1 (gold) and terminal Fe/Co2 sites (green) are distinguished. (b) Refined average coordination environment (at 443 K) of the central transition metal Fe/Co1 site in the trilayer in **III**. The blue spheres represent the residual 8% occupancy of the original equatorial O5 oxide sites. The purple spheres represent the 5.5% occupied O4 sites. Axial O2 oxygens are 100% occupied. All atoms are represented by thermal ellipsoids at the 50% probability level. (c) Local environment of the transition metal sites in **III** deduced from the average scattering density (at 443 K). The light and dark purple O4 positions are consistent with occupancy of the central Fe/Co1 site by Co²⁺ and Fe²⁺, respectively. The coordination at the flanking Fe/Co2 site is assigned as square-based pyramidal.

the metal content is unchanged from **I**. Electron diffraction confirms that the *I4/mmm* space group is retained (Figure 2 inset).

Rietveld analysis of neutron powder diffraction data (collected at 443 K to suppress magnetic scattering) demonstrates that the equatorial O5 anion site at the central BO₆ octahedron (corresponding to four in-plane oxide neighbors) is vacant, which would place the central Fe/Co1 cations in a linear two-coordinate environment – removing O5 improves the goodness-of-fit parameter χ^2 from 3.9 to 1.2. Difference Fourier calculations at this stage reveal an extra disordered oxide 16l (*x,y,0*) anion site (O4) displaced by 0.95 Å in the *ab* plane from O5, with a refined occupancy of 5.5(5)% (Figure 1c). The improvement in the match with the observed intensities permitted the location of residual scattering density on the original equatorial oxide O5 position in the central layer, corresponding to 8.1% occupancy (final χ^2 = 1.06, Figure S4). The refined Sr₃LaFe_{1.5}Co_{1.5}O_{7.5(1)} composition agrees with the TG determination. The environment of the central Fe/Co1 site in the trilayer is interesting (Figure 1b). The two axial Fe/Co1–O2 bonds at 1.787(7) Å are exceptionally short for Fe²⁺ or Co²⁺, reflecting the increase in bonding required to compensate for the low coordination number of the site. The equatorial coordination to Fe/Co1 is provided by 16 disordered O4 positions (which are approximately 1/16 occupied), plus 8% occupancy of the original O5 0,1/2,0 positions. This corresponds to 68% of the metal centers having only one O4 site and none of the original O5 oxide sites within their coordination sphere. Electron diffraction (Figure 2 inset)

[†] University of Liverpool.

[‡] Laboratoire CRISMAT-ENSICAEN.

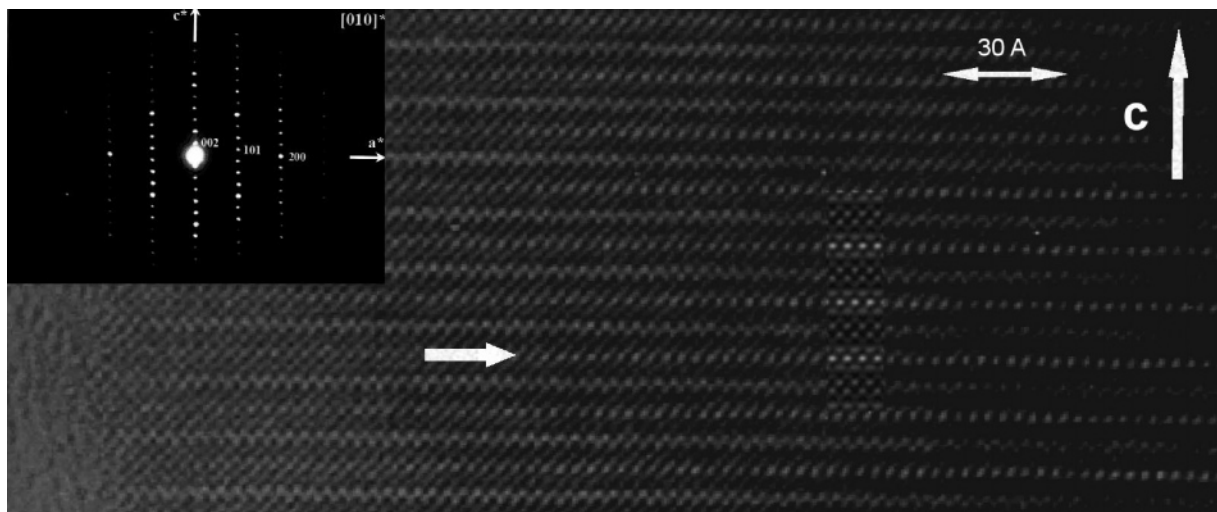


Figure 2. Experimental electron diffraction pattern and HREM image of **III** recorded along the $[100]_p$ direction with inset simulated image (calculated for a defocus value close to -250 Å and a thickness of 50 Å).

shows no ordering of the disordered anion positions refined from the neutron data.

HREM lattice images of **III** reveal the retention of the three-layer stacking sequence. In the thicker part of the crystal, bright dots are observed in the central BO_2 layer (white arrow in Figure 2). Taking into account their intensity compared to those observed in the $[\text{La}/\text{SrO}]$ rock-salt-type layers and the experimental defocus close to the Scherzer value, these contrasts are correlated with the expected rows of anion vacancies from the structural model. HREM image simulation from the refined atomic positions and site occupancies (inset in Figure 2) fits well with the experimental image.

The site disorder around $\text{Fe}/\text{Co}1$ in the equatorial plane can be resolved locally by focusing on the 68% of metal sites which have a single $\text{O}4$ neighbor (Figure 1c). There are two distinct $\text{Fe}/\text{Co}1-\text{O}4$ bond lengths—the longer contact of $2.38(4)$ Å gives a bond valence of 1.9 for Fe and 1.7 for Co, while the shorter contact of $1.95(4)$ Å gives 2.04 for Co and 2.3 for Fe, consistent with assignment of the shorter $\text{Fe}/\text{Co}1-\text{O}4$ contact to occupancy of the site by Co^{2+} and the longer by Fe^{2+} . The limitations of the bond valence sum treatment in disordered materials should be borne in mind here, but it is clear that the low oxidation state at the B site for Fe and Co is thus stabilized because the required low coordination number can be compensated by shortening of the axial contacts to the flanking octahedral layers. The unusual three-coordinate environment for the Fe^{2+} and Co^{2+} cations in the heavily reduced **III** is thus stabilized within the extended connectivity of the perovskite-derived structure: this extended network is essential for both ionic and electron transport. Three-coordinate Fe^{2+} has been observed in isolated $[\text{Fe}_2\text{O}_5]^{6-}$ anions in orthoferrates with an equilateral triangular geometry.⁶ The anisotropic displacement parameters of $\text{Fe}/\text{Co}1$ are twice as large in the ab plane as along c , which would permit local displacements ($\text{rms} = 0.2$ Å) to shorten equatorial $\text{Fe}/\text{Co}1-\text{O}4$ and lengthen axial $\text{Fe}/\text{Co}1-\text{O}2$ bonds.

The mean coordination number at the terminal $\text{Fe}/\text{Co}2$ sites in the trilayer is 5. The 75% occupancy of the equatorial $\text{O}1$ site is

consistent with a disordered square-based pyramidal coordination at Fe2 (Figure 1c), with the vacant site occupying one of four possible positions. Other interpretations of the observed scattering density are discussed in the Supporting Information.

The behavior of $\text{Sr}_3\text{LaFe}_{1.5}\text{Co}_{1.5}\text{O}_{10}$ on reduction reveals that this structure type is able to tolerate both low metal oxidation states and unusual coordination numbers—Fe and Co are commonly found in four- to six-coordinate sites in extended oxides with structures associated with mixed conduction, and Fe^{3+} perovskites are rarely reducible to pure Fe^{2+} systems. This may be important in understanding the behavior of these materials in extreme, possibly nonequilibrium, conditions found in gas separation membranes and fuel cell environments. Three-coordinate metal centers may also be involved in oxide mobility mechanisms in such systems.

Acknowledgment. We thank the UK EPSRC for support (EP/C511794/1) and access to the Daresbury SRS and ILL, where we thank Dr. M. A. Roberts (SRS) and Dr. P. F. Henry (ILL) for assistance. D.P. thanks the FAME fellow exchange program.

Supporting Information Available: Experimental details for synthesis, powder diffraction (CIF), TGA, XAS, TEM, and HREM. This material is available free of charge via the Internet at <http://pubs.acs.org>.

References

- (1) Huang, Y. H.; Dass, R. I.; Xing, Z. L.; Goodenough, J. B. *Science* **2006**, *312*, 254–257.
- (2) Wang, S.; van der Heide, P. A. W.; Chavez, C.; Jacobson, A. J.; Adler, S. B. *Solid State Ionics* **2003**, *156*, 201–208.
- (3) Li, Y. P.; Maxey, E. R.; Richardson, J. W. *J. Am. Ceram. Soc.* **2005**, *88*, 1244–1252.
- (4) Armstrong, T.; Prado, F.; Manthiram, A. *Solid State Ionics* **2001**, *140*, 89–96.
- (5) Hayward, M. A.; Cussen, E. J.; Claridge, J. B.; Bieringer, M.; Rosseinsky, M. J.; Kiely, C. J.; Blundell, S. J.; Marshall, I. M.; Pratt, F. L. *Science* **2002**, *295*, 1882–1884.
- (6) Müller, H. P.; Hoppe, R. Z. *Anorg. Allg. Chem.* **1993**, *619*, 193–201.

JA064083G